



Statistical modeling for forecasting land surface temperature increase in Taiwan from 2000 to 2023 using three knots cubic spline

Abdulmana, S., Prasetya, T. A. E., Garcia-Constantino, M., & Lim, A. (2024). Statistical modeling for forecasting land surface temperature increase in Taiwan from 2000 to 2023 using three knots cubic spline. *Modeling Earth Systems and Environment*, 10(2), 2793-2801. <https://doi.org/10.1007/s40808-023-01926-9>

[Link to publication record in Ulster University Research Portal](#)

Published in:
Modeling Earth Systems and Environment

Publication Status:
Published (in print/issue): 30/04/2024

DOI:
[10.1007/s40808-023-01926-9](https://doi.org/10.1007/s40808-023-01926-9)

Document Version
Author Accepted version

General rights

The copyright and moral rights to the output are retained by the output author(s), unless otherwise stated by the document licence.

Unless otherwise stated, users are permitted to download a copy of the output for personal study or non-commercial research and are permitted to freely distribute the URL of the output. They are not permitted to alter, reproduce, distribute or make any commercial use of the output without obtaining the permission of the author(s).

If the document is licenced under Creative Commons, the rights of users of the documents can be found at <https://creativecommons.org/share-your-work/cclicenses/>.

Take down policy

The Research Portal is Ulster University's institutional repository that provides access to Ulster's research outputs. Every effort has been made to ensure that content in the Research Portal does not infringe any person's rights, or applicable UK laws. If you discover content in the Research Portal that you believe breaches copyright or violates any law, please contact pure-support@ulster.ac.uk

Statistical Modeling for Forecasting Land Surface Temperature increase in Taiwan from 2000 to 2023 using three knots cubic spline

Sahidan Abdulmana, Tofan Agung Eka Prasetya, Matias Garcia-Constantino and Apiradee Lim

Abstract

Taiwan is highly mountainous, making it the world's fourth-highest island. The main island is distinguished by the contrast between its eastern two-thirds, which consist primarily of rough forest-covered mountains. Taiwan's climate is influenced by the east Asian monsoon, whereas regions of central and southern Taiwan have a tropical monsoon climate. Climate change is causing the monsoon to become increasingly irregular, unreliable, and even deadly, with more severe rainfall and worsening dry spells. Land surface temperature (LST) is an essential parameter because the warmth rising off Earth's landscapes influences our world's weather and climate patterns. Therefore, the objectives of this study are: (i) to investigate the daytime LST annual seasonal patterns and trends, and (ii) to forecast LST increase in sub-regions and regions in Taiwan. The data used in this study was time series data of daytime LST from 2000 to 2023 from the Moderate Resolution Imaging Spectroradiometer (MODIS) website. The natural cubic spline method with eight knots was used to investigate the annual seasonal patterns of daytime LST. The linear regression model was applied to model the LST trends, and a cubic spline with 2, 3, and 4 knots was then applied to forecast LST trends over 23 years. Moreover, the multivariate regression model was used to adjust the spatial correlation and to evaluate the increase in daytime LST. The results demonstrate that daytime LST in Taiwan has increased on average by 0.151 °C per decade. Most of the daytime LST by sub-regions had a consistent increase. Furthermore, daytime LST in all regions had increasing trends. Using three knots of cubic spline to forecast daytime LST trends illustrates the significant increase trends compared with other spline knots. In conclusion, daytime LST in Taiwan is gradually increasing and the reasons for these trends toward daytime LST need to be explored in future studies.

Keywords: Land surface temperature, three knots cubic spline function, linear regression, multivariate regression model

Introduction

At the local and global levels, the temperature is one of the key indicators in climate research. One method for measuring temperature in a place is to measure Land Surface Temperature (LST). LST is the ground temperature of the earth's surface resulting from land surface-atmosphere interactions and energy fluxes between the surface and the atmosphere (Khandelwal et al. 2018). Identifying the changing dynamics of LST on a regional scale is a highly convenient technique to discuss the concerns associated with global warming and climate change. Other key advantages of monitoring LST in key climatic region is to better understand environmental problems and their impact on human life sustainability (Esha and Rahman 2021). Furthermore, it has the potential to significantly alter the seasonal vegetation index phenology, which effects the local and global energy balance (Islam and Ma 2018). LST has increased in several parts of the world (Mustafa et al. 2020; Fitra-hanjani et al. 2021; Abdulmana

et al. 2021, Wang et al. 2022; De Almeida et al. 2023), for instance, Lean and Rind (2009) discovered that from 2009 to 2019 the global LST was influenced by human activities (e.g. anthropogenic effect, solar irradiance, and volcanic aerosols) and had steadily increased. Nevertheless, it is a tool for investigating climate change on the ground surface.

Previous studies have applied several different statistical modeling techniques to generate models and to forecast LST trends. Wanishsakpong and McNeil (2016) produced spatial correlations using factor analysis and a sixth-order polynomial regression model to predict the patterns and trends of LST. However, the polynomial regression model mainly depended on the time period and features of the data used. Wongsai et al. (2017) applied natural cubic spline model to investigate seasonal daytime LST patterns in Phuket Island, Thailand, and noted that global temperatures are dynamic and that it is difficult to control their undesirable consequences. In another research study (Abdulmana et al. 2022), a linear regression model and four knots cubic spline were applied to illustrate the LST trends in Taiwan. In (Kesavan et al. 2021), Autoregressive Integrated Moving Average (ARIMA) model was applied to estimate and forecast LST in Tamil Nadu state of India. Mustafa et al. (2020) applied Dynamic Evolving Neuro Fuzzy Inference System (DENFIS), Adaptive Neuro Fuzzy Inference System (ANFIS), Wavelet Neural Network (WNN), and Multivariate Adaptive Regression Splines (MARS) to investigate the effective model that could be utilized to forecast the alteration of LST in the Beijing region. They found that the ANFIS model was the highest performance prediction model in the training and testing stages of LST with the highest r-square.

Therefore, many previous studies have considered modeling and forecasting LST seasonal patterns and trends with diverse methodologies. There were a few studies focusing on forecasting LST trends using a cubic spline with a suitable knot (Wongsai et al. 2017; Abdulmana et al. 2022). In addition, some studies on variations of daytime LST have covered large areas of mainland countries; however, there were some works focusing on Urban Heat Island (UHI), of which Taiwan is one example. The population and urbanization in Taiwan have increased rapidly since 1967 and has been affected by temperature variations (Lai and Cheng 2010). Additionally, the growth of urbanization is an important factor in regional and global development and could impact local climate change. The study presented explores the daytime LST annual seasonal patterns and forecasts LST trends with an appropriate knot of cubic spline in Taiwan from 2000 to 2023. The remainder of this paper is organized as follows: Section 2 presents the materials used and the proposed method. Section 3 presents and describes the results obtained, and Section 4 discusses the results. Finally, Section 5 presents the conclusions.

Materials and Method

Study area

Taiwan is a small island with a land area of 35,980 km² (World Data 2022) that has mountains and foothills covering over two-thirds of the island. In the analysis of this study, the Taiwan area was divided into four regions following Taiwan's thematic map (northern, central, eastern, and southern regions), with nine sub-regions in each region. Therefore, the total number of sub-regions considered for the analysis is 36, as illustrated in (Fig. 1). The Google Earth software was used to retrieve the coordinates of each sub-region. The MODIS Land (MODLAND) tile calculator website was used to avoid overlap between sub-regions and to assign the longitude and latitude for

getting the tile vertical and horizontal coordinates, sample, and line numbers. The area of each sub-region is 7×7 km², which equals to 49 pixels in a 1×1 km² grid. The total pixels were 1,764 in the whole study area.

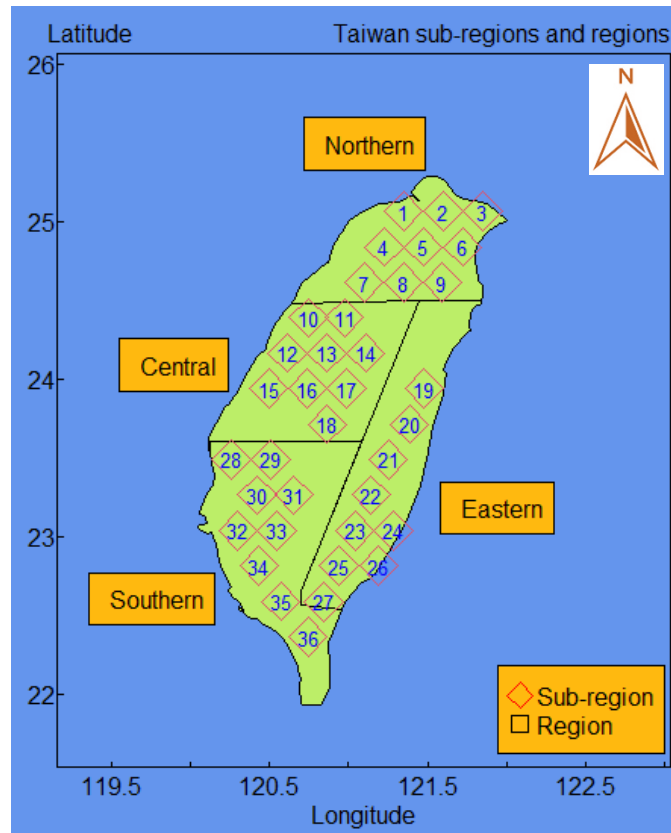


Fig. 1 Taiwan map showing 4 regions with 36 sub-regions

Data source

Daytime LST data were downloaded from the MODIS emissivity eight-day composite global dataset for every 1 km, with the daytime records covering the period from March 2000 to June 2023. Each year, there are 45 observations per grid cell, thus the observations total number is 1,035 over 23 years. The dataset used in this study is called MODIS/Terra LST and Emissivity LST (MOD11A2).

Seasonal patterns and adjusted time series

Daytime LST time series data normally include seasonality as another time series data. However, in order to model LST patterns and trends over 23 years, the daytime LST time series should be adjusted for seasonality. The natural cubic spline function with definite boundary conditions was applied to ensure smoothness over the period of daytime LST in each sub-region. This model has been applied by many previous studies in areas including Phuket Island, Thailand (Wongsai et al. 2017), Nepal (Sharma et al. 2018), Peninsular Malaysia (Ismail et al. 2019), and Taiwan (Abdulmana et al. 2021, Abdulmana et al. 2022). The eight knots of a cubic spline were assigned and fit to the data in this model for the Julian days 10, 40, 80, 130, 240, 290, 330, and 360. The formula takes the form:

$$\hat{y}_t = a + bt + \sum_{k=1}^p c_k (t - t_k)_+^3 \quad (1)$$

where \hat{y}_t is the model predicted daytime LST and a , b and c_k are the coefficients used to fit the model. k is the location of the knot; p is the total number of knots and t indicates the time in Julian days, which is used to identify the day of the year. $t_1 < t_2 < \dots < t_p$ are indicated knots and $(t - t_k)_+$ is positive for $(t > t_k)$ and zero otherwise.

Then, the seasonally adjusted time series was computed by placing the original values and subtracting them from the predicted patterns and adding the values of the mean to verify that the average daytime LST over the period of 23 years was unchanged. The formula takes the form:

$$y_{sa} = y - \hat{y}_t + \bar{y} \quad (2)$$

where, y_{sa} is the seasonally adjusted daytime LST, y is the original value subtracted with \hat{y}_t which is the fitted value, plus the overall mean \bar{y} of observed data.

Forecasting LST trends

To forecast LST trends over 23 years, the study applied 2, 3, and 4 knots of spline function to observe the suitable knot for forecasting. The knots cover the range of the data, therefore, extreme knots correspond to the minimum and maximum time points, respectively. The natural spline, which is linear beyond the range of the data, was applied with two boundary conditions needed to make the function linear outside the data range, the formula is as follows:

$$y = a + bx + \sum_{k=1}^{p-2} c_k s_k(x), \quad (3)$$

Where $s_k(x) = (x - x_k)_+^3 \frac{(x_p - x_k)}{d} (x - x_{p-1})_+^3 + \frac{(x_{p-1} - x_k)}{d} (x - x_p)_+^3$, $d = x_p - x_{p-1}$ and $x_+ = x$ if $x > 0$, 0 otherwise.

The formula of a two knots spline is $y = a + bx$, which is just a straight line. In the case of three knots, the spline has three parameters, like a quadratic function, but this function is more useful in practice because its forecasts are linear, whereas forecasts based on quadratics tend to overshoot or undershoot data. Splines with more than three knots, can detect periodic waves in data and might provide better short-term forecasts, however they are less accurate for long-term forecasts because they tend to increase or decrease too rapidly. With $p = 3$, the formula is $y = a + bx + c_1 s_1(x)$, where, after doing some algebra calculations, we obtain:

$$S_1(x) = x_1 \{ (x_2^2 + x_2 x_3 + x_2^2 - x_2 x_3 (x_2 + x_3) - x_1^3) + 3c_1 (x_2 - x_1)(x_3 - x_1) x \text{ for } x > x_3 \} \quad (4)$$

Formula 4 describes that before the first knot (x_1), y would increase at rate b , whereas after the last knot (x_3), y would increase at rate $b + 3c_1(x_2 - x_1)(x_3 - x_1)$. Consequently, the increase in slope over the range of the data ($x_3 - x_1$) is $3c_1(x_2 - x_1)(x_3 - x_1)$. Accordingly, the average acceleration over the data range is $3c_1(x_2 - x_1)$.

Auto Regressive Integrated Moving Average (ARIMA) model was applied to detect the temporal autocorrelation from the model. The first and second ARIMA order autoregressions were applied. The daytime LST trends from ARIMA models of each sub-region were demonstrated in a time series plot. Additionally, the increase of the daytime LST by regions was illustrated on the Taiwan map to show 23 years of the daytime LST variations. As most of the time series variables are spatially correlated, it was necessary to handle them estimating

the average increases of daytime LST by regions applying a multivariate regression model. The confidence interval of the increase of daytime LST and the acceleration increase of daytime LST per decade were illustrated using a forest plot. The R software was used for all statistical analyses and plots (R Core Team 2018).

Results

Daytime LST annual seasonal patterns over 23 years

The fitting cubic spline function with eight knots is illustrated in (Fig. 2). The reason for selecting eight knots was because they gave the highest r square. In this study, the annual seasonal pattern plots of all the sub-regions in Region 2 have been chosen to display the patterns. The Y axis represents Daytime LST in degree Celsius ($^{\circ}\text{C}$), and the X axis shows the day of the year.

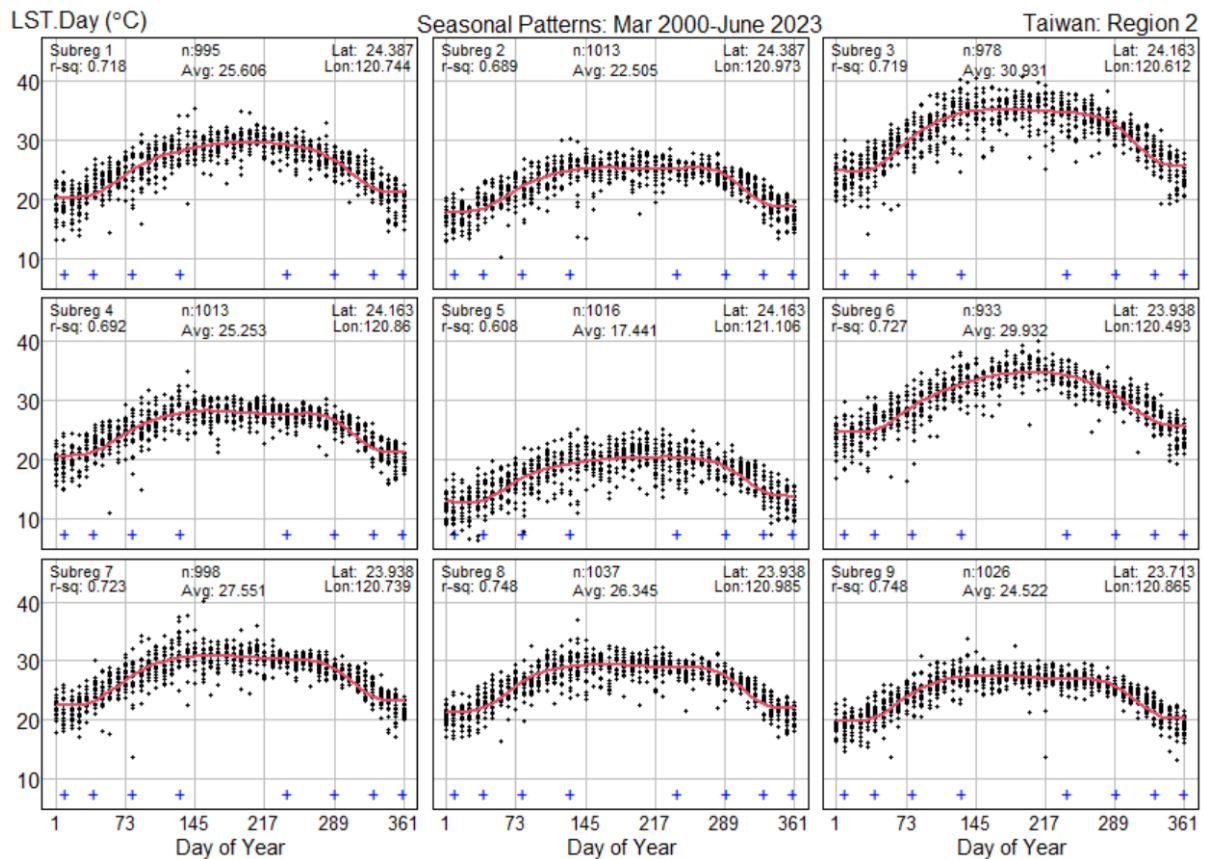


Fig. 2 Seasonal pattern of Daytime LST in Region 2 with 9 sub-regions

Fig. 2 illustrates the annual seasonal patterns fitted by the natural cubic spline functions with eight knots, denoted by a blue plus sign. These nine plots represent the daytime LST of the nine sub-regions in Region 2, which is in the central area of Taiwan. Vertical stacks of points denote average surface temperatures for eight-day periods (the orbital period of the Terra satellite is eight days) recorded during 23 years from 18 February 2000 to 30 June 2023 based on 46 orbits per year. The values of n denote the total number of observations. There was a steady increase in daytime LST in March with a peak in July. From September there was a moderate decrease with the lowest point being achieved in winter from December to February. There was a similar annual seasonal pattern of LST for other sub-regions and regions for each year.

Fitted model for forecasting LST trend over 23 years

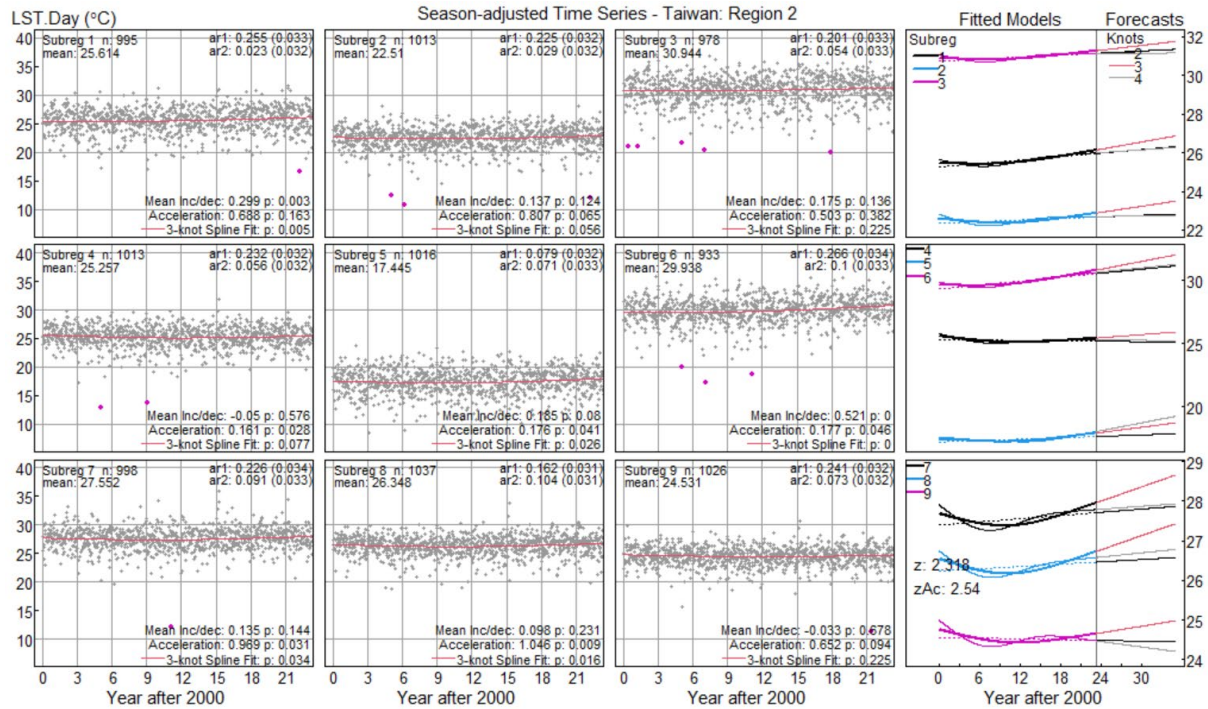


Fig. 3 Time series trends for corresponding seasonally-adjusted daytime LST, fitted model and forecasting in Region 2 with 9 sub-regions

Note that in (Fig. 3) n is the number of observations, ar1 is the first order autoregression, ar2 is the second order autoregression, mean is the mean daytime LST over 23 years, Mean Inc/dec is the mean Daytime LST increase per decade, Acceleration is the accelerated increase, p is the p-value, z is the z value, zAc is the acceleration value, and knots is the number of forecasting knot.

Fig. 3 shows the trends of daytime LST from 2000 to 2023 from ARIMA models based on cubic spline function in the central region of Taiwan. Ar1 and ar2 represent the first and second-order autoregressive values from using the ARIMA model, respectively. Curves in the three plots in the fourth column show fitted models and forecasting of each three sub-regions in each row. Furthermore, 2, 3, and 4 knots were used for the forecasting trends. The results by sub-regions show diverse LST trends, for instance, Sub-region 3 in Region 2 had the highest mean daytime LST, which was 30.944 °C, while Sub-region 5 had the lowest mean daytime LST with 17.445 °C. However, there was a significant increasing trend of LST over 23 years by fitting the model for forecasting with three knots cubic spline and more accurate results compared to other knots. The p-values and the mean increases per decade were used to estimate the LST increase of the daytime by sub-region, as summarized in (Table 1). In addition, the z value in the bottom right panel of (Fig. 3) was used to estimate the LST increase of the daytime by region, as summarized in (Table 2).

Table 1 Mean increase/decade of the daytime LST with p-values for 36 sub-regions in Taiwan from 2000 to 2023

Variable			Variable		
LST			LST		
Sub-region	Increase	P-value	Sub-region	Increase	P-value
1	0.080	0.530	19	0.056	0.626
2	0.287	0.049	20	-0.016	0.872
3	0.118	0.473	21	0.362	0.007
4	0.056	0.642	22	0.271	0.032
5	0.025	0.823	23	0.262	0.027
6	0.083	0.492	24	-0.183	0.068
7	0.039	0.682	25	0.333	<0.001
8	0.099	0.314	26	-0.348	<0.001
9	0.122	0.232	27	0.739	0.000
10	0.299	0.003	28	0.123	0.371
11	0.137	0.124	29	0.204	0.031
12	0.175	0.136	30	0.153	0.092
13	-0.050	0.576	31	0.132	0.106
14	0.185	0.080	32	0.362	<0.001
15	0.521	0.000	33	-0.086	0.342
16	0.135	0.144	34	-0.049	0.597
17	0.098	0.231	35	0.465	0.000
18	-0.033	0.678	36	0.294	0.002

Table 2 95% CI (Confidence Interval) of the daytime LST increases and z-values of each region from 2000 to 2023

Variable		LST	
		95% CI	
Region	Increase	(Confidence Interval)	z-value
Northern	0.101	-0.136 - 0.338	1.35
Central	0.161	-0.025 - 0.351	2.318
Eastern	0.162	-0.058 - 0.386	2.125
Southern	0.176	-0.015 - 0.370	2.598
Average	0.151	-0.009 - 0.291	

Daytime LST change by sub-region and region over 23 years

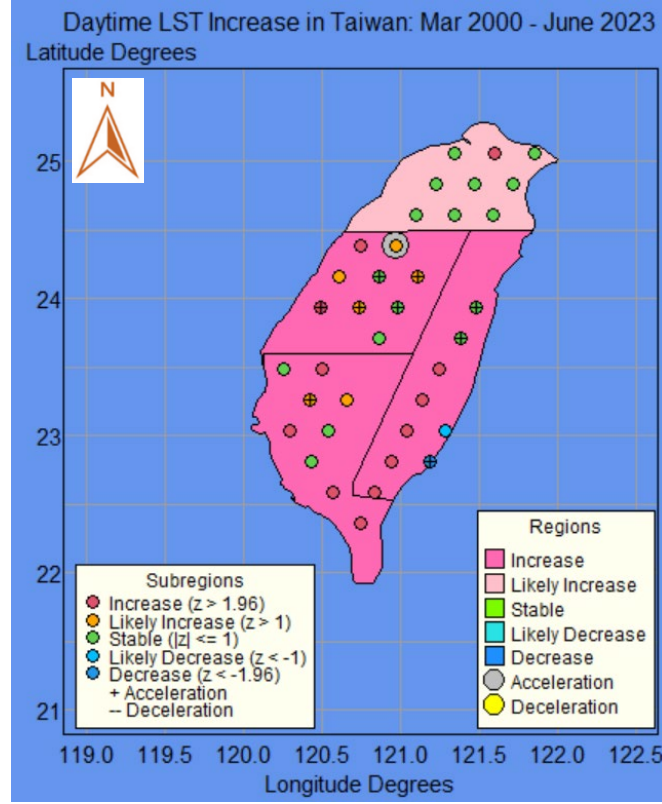


Fig. 4 Daytime LST changes by sub-regions and regions in Taiwan from 2000 to 2023

Fig. 4 demonstrates the daytime LST variation in the sub-regions and regions of Taiwan. The legends at the bottom left and right illustrate the changes of the daytime LST in diverse colors by sub-regions and regions over 23 years. The decadal mean increase values and p-values of each sub-region are derived from (Table 1), and they were used to describe the decrease and increase in daytime LST in the sub-regions. If the increase value > 0 and p-value < 0.05 , this was specified as increase (red); if the increase > 0 and p-value < 0.159 , this was indicated as likely increase (orange); if increase < 0 and p-value < 0.159 was specified as likely decrease (light blue); if increase < 0 and p-value < 0.05 , this was indicated as decrease (blue); and the remaining condition was indicated as stable (green). The decreasing and increasing values of each region and z-value were derived from (Table 2). Z-values were used to specify the decrease and increase levels. If the z-values of daytime LST > 1.96 , this was indicated as increase (red); if the values > 1 to 1.96 , this was indicated as likely increase (orange); if the values ≤ 1 , this was indicated as stable (green); if the values < -1 to -1.96 , this was indicated as likely decrease (light blue); and if the values < -1.96 , this was indicated as decrease (blue). The brown color is indicated as acceleration and the yellow color is indicated as a deceleration in the region. The results show that most of the daytime LST by sub-regions were stable, except for Sub-regions 3, 10, 15, 21, 22, 23, 25, 17, 29, 32, 35, and 36, which had significantly increased daytime LST. There was an increase in the daytime LST in all regions. Consequently, decadal increase

and 95% confidence interval values were used to estimate the decadal of daytime LST increase by region, as summarized in (Table 2).

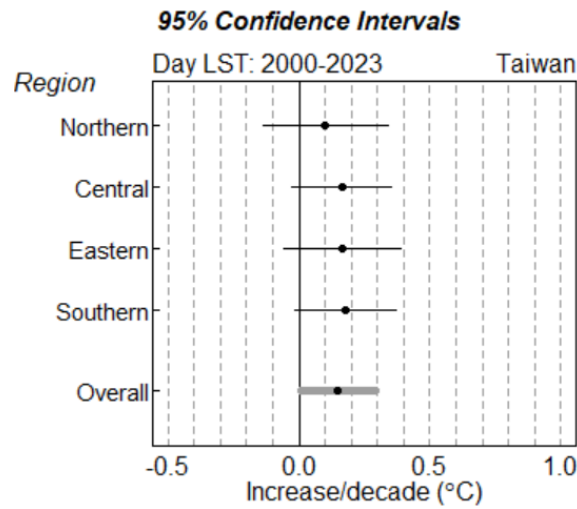


Fig. 5 95% Confidence Intervals of decadal daytime LST increases from 2000 to 2023

Fig. 5 presents the range of the 95% confidence intervals of daytime LST increases per decade using a forest plot. The particular region is represented in the Y axis, which comprises four regions: northern, central, eastern, and southern region. The daytime LST increase per decade is demonstrated in the X axis. The plot shows an increasing decadal daytime LST in all regions, with the southern region showing the highest increase per decade (0.176 °C). The average increase per decade was 0.151 °C.

Discussion

Using a proper number of cubic spline knots and linear regression could effectively extract yearly daytime LST seasonal patterns and trends. This study used an eight knots of cubic spline method to model daytime LST seasonality, which was a similar method to previous related works (Wongsai et al. 2017; Sharma et al. 2018; Ismail et al. 2019; Abdulmana et al. 2021; Abdulmana et al. 2022; Munawar et al. 2022). The average increase in daytime LST was 0.151 °C per decade, which indicates the rising trend of daytime LST and its consistency with many previous studies (Wongsai et al. 2017; Islam and Ma 2018; Hamoodi et al. 2019; Mustafa et al. 2020; Fitrahanjani et al. 2021). Additionally, our study supports the results from the Council for Economic Planning and Development in Taiwan, which reported that Taiwan's annual temperature had increased by 0.29 °C per decade (1980-2009) (Council for Economic Planning and Development 2012). According to Chan and Chan (2023) stated there was an increasing LST trend at 0.031 °C per year from 2000 to 2022 at kueishantao (KST) volcano of Taiwan.

Forecasting trends with 2, 3 and 4 knots cubic spline

This study used 2, 3, and 4 knots cubic spline to forecast daytime LST increase, as displayed in (Fig. 6). The use of the three knots spline function (red line) was an effective approach to forecast LST for a short period because

it produced a significant increase compared to other knots. However, while it is useful in practice because its forecasts are linear, it is not suitable for long-term forecast because it rapidly tends to increase or decrease.

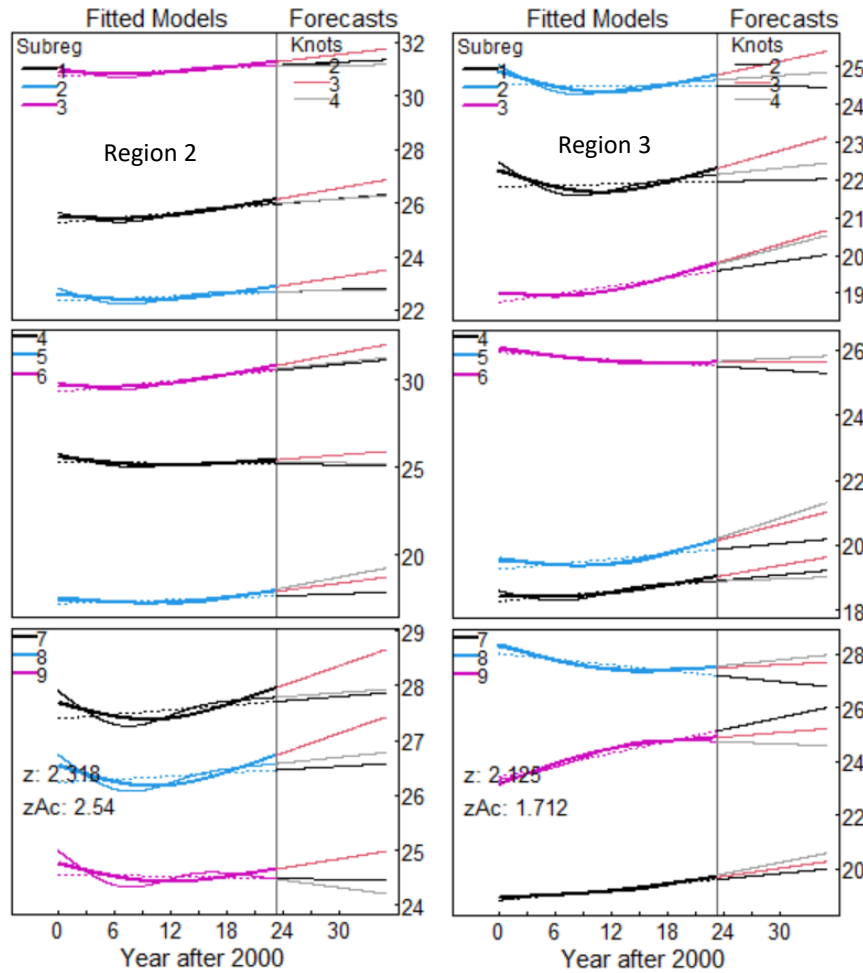


Fig. 6 Fitted model and forecasting trends of cubic spline

Many previous studies applied different forecasting techniques with time series data. Abdulmana et al. (2021) applied zero and four knots of cubic spline to estimate linear and forecast LST trends. While zero knot is indicated as linear regression, with the use of four knots spline it was not mentioned the significant effectiveness of the forecasting. In the approach presented by Kesavan et al. (2021), an ARIMA-based model was applied to forecast LST in the metropolitan city of Chennai, China. They found that the accuracy of the ARIMA model for forecasting is unitized for short-term input data.

The regression analysis model is the mutual statistical method for forecasting LST and UHI (Chun and Guldmann 2014), for instance, spectral analysis, cluster analysis, correlation analysis, factor analysis, principal analysis (Wang et al. 2019), weighted regression analysis (Su et al. 2012). Therefore, most of the analysis that use regression are not sufficiently effective for non-linear data (Wang et al. 2019). Ustaoglu et al. (2008) applied an Artificial Neural Network (ANN) model to forecast temperature with high forecasting accuracy. Moreover, Multivariate Adaptive Regression Splines (MARS), Dynamic Evolving Neurofuzzy Inference System (DENFIS), and Adaptive Neurofuzzy Inference System (ANFIS) could be used to predict the LST in Beijing, China (Mustafa et al. 2020).

Conclusion

The results of the analysis presented supports our proposed method for modeling and forecasting time series data with spatial and temporal alterations of daytime LST. The study found that there was an increase in the mean of daytime LST per decade in almost all sub-regions except for Sub-regions 24 and 26, in which there was a decrease. Furthermore, the regional level shows an increasing trend in all regions. Daytime LST in Taiwan has increased in the last two decades and continues to increase, with an average increase in daytime LST of 0.151 per decade. The increasing surface temperature is affected by urban expansion and farmers, especially in the southern region, which is an agricultural area. This rise could be used to warn Taiwan's policymakers to have better planning to deal with future global warming.

The forecasting trends using three knots of cubic splines presented in this study indicated that daytime LST in Taiwan has been rising. Moreover, it also showed that three knots of cubic spline is a suitable knot for forecasting daytime LST as demonstrated in this analysis with the reasonably high accuracy obtained. However, something to consider when applying this method is that a cubic spline with three knots is appropriate for short-term forecasts. Therefore, the increasing trends in daytime LST are a result of the rapid growth of Taiwan's economy and its industrialization, which have increased energy consumption.

Acknowledgements

This publication is based on work supported by Airlangga Post-Doctoral (APD) Fellowship Program, Ref. No: 257/UN3.22/KS/2023. We acknowledge the Department of Data Science and Analytics, Fatoni University, for providing facilities for this study. We are grateful to Professor Don McNeil for his immense guidance during the research.

Data availability All data generated or analyzed during this study can be obtained from the corresponding author.

Declarations

Conflict of interest The authors declare that they have no conflict of interest.

References

- Abdulmana S, Lim A, Wongsai S, Wongsai N (2021) Land surface temperature and vegetation cover changes and their relationships in Taiwan from 2000 to 2020. *Remote Sens Appl: Soc Environ* 24:100636. <https://doi.org/10.1016/j.rsase.2021.100636>
- Abdulmana S, Lim A, Wongsai S, Wongsai N (2022) Effect of land cover change and elevation on decadal trend of land surface temperature: a linear model with sum contrast analysis. *Theor Appl Climatol* 1-12. <https://doi.org/10.1007/s00704-022-04038-z>

- Chan HP, Chan YC (2023) Thermal pattern at Kueishantao (KST) volcano of Taiwan from satellite-observed temperatures and its implication. *Environ res commun* 5(7):075013. <https://doi.org/10.1088/2515-7620/ace760>
- Chun B, Guldmann JM (2014) Spatial statistical analysis and simulation of the urban heat island in high-density central cities. *Landsc Urban Plan* 125:76–88. <https://doi.org/10.1016/j.landurbplan.2014.01.016>
- Council for Economic Planning and Development (2012) Adaptation strategy to climate change in Taiwan. Taipei, 1st edition. ISBN: 978-986-03-3755-6
- De Almeida CR, Garcia N, Campos JC, Alirio J, Arenas-Castro S, Gonçalves A, Teodoro AC (2023) Time-series analyses of land surface temperature changes with Google Earth Engine in a mountainous region. *Heliyon*, 9(8). <https://doi.org/10.1016/j.heliyon.2023.e18846>
- Esha E, Rahmad MTU (2021) Simulation of future land surface temperature under the scenario of climate change using remote sensing & GIS techniques of northwestern Rajshahi district, Bangladesh. *Environ Chall* 5. <https://doi.org/10.1016/j.envc.2021.100365>
- Fitra-hanjani C, Prasetya TAE, Indawati RA (2021) Statistical method for analysing temperature increase from remote sensing data with application to Spitsbergen Island. *Model Earth Syst Environ* 7:561–569. <https://doi.org/10.1007/s40808-020-00907-6>
- Hamoodi MN, Corner R, Dewan A (2019) Thermophysical behaviour of LULC surfaces and their effect on the urban thermal environment. *J Spat Sci* 64(1):111-130. <https://doi.org/10.1080/14498596.2017.1386598>
- Islam S, Ma M (2018) Geospatial monitoring of land surface temperature effects on vegetation dynamics in the Southeastern Region of Bangladesh from 2001 to 2016. *ISPRS Int J Geo-Inf* 7(12):486. <https://doi.org/10.3390/ijgi7120486>
- Ismail NA, Zin WZW, Ibrahim W, Yeun LC (2019) Eight-day daytime land surface temperature pattern over peninsular Malaysia. *Int J Eng Technol* 8:11949-11955. <https://doi.org/10.35940/ijrte.D9911.118419>
- Kesavan R, Muthian M, Sudalaimuthu K, Sundarsingh S, Krishnan S (2021) ARIMA modeling for forecasting land surface temperature and determination of urban heat island using remote sensing techniques for Chennai city, India. *Arab J Geosci* 14(11):1-14. <https://doi.org/10.1007/s12517-021-07351-5>
- Khandelwal S, Goyal R, Kaul N, Mathew A (2018) Assessment of land surface temperature variation due to change in elevation of area surrounding Jaipur, India. *Egypt J Remote Sens Space Sci* 21(2018):87–94. <https://doi.org/10.1016/j.ejrs.2017.01.005>
- Lai LW, Cheng WL (2010) Air temperature change due to human activities in Taiwan for the past century. *Int J Climatol: A J R Meteorol Soc* 30(3):432-444. <https://doi.org/10.1002/joc.1898>
- Lean JL, Rind DH (2009) How will Earth's surface temperature change in future decades? *Geophys Res Lett* 36(15). <https://doi.org/10.1029/2009GL038932>

- Munawar M, Prasetya TAE, McNeil R, Jani R (2022) Statistical modeling for land surface temperature in Borneo island from 2000 to 2019. *Theor Appl Climatol* 1-8. <https://doi.org/10.1007/s00704-021-03891-8>
- Mustafa EK, Co Y, Liu G, Kaloop MR, Beshr AA, Zarzoura F, Sadek M (2020) Study for predicting land surface temperature (LST) using landsat data: a comparison of four algorithms. *Adv Civ Eng* 2020. <https://doi.org/10.1155/2020/7363546>
- R Core Team R (2018) A language and environment for statistical computing, R foundation for statistical computing, Vienna, Austria.
- Sharma I, Tongkumchum P, Ueranantasun A (2018) Modeling of land surface temperatures to determine temperature patterns and detect their association with altitude in the Kathmandu Valley of Nepal. *Chiang Mai University J Nat Sci* 17(4). <https://doi.org/10.12982/CMUJNS.2018.0020>
- Su YF, Foody GM, Cheng KS (2012) Spatial non-stationarity in the relationships between land cover and surface temperature in an urban heat island and its impacts on thermally sensitive populations. *Landsc Urban Plan* 107:172–180. <https://doi.org/10.1016/j.landurbplan.2012.05.016>
- Ustaoglu B, Cigizoglu H, Karaca M (2008) Forecast of daily mean, maximum and minimum temperature time series by three artificial neural network methods. *Meteorol Appl* 15:431–445. <https://doi.org/10.1002/met.83>
- Wang H, Huang J, Zhou H, Zhao L, Yuan Y (2019) An integrated variational mode decomposition and ARIMA model to forecast air temperature. *Sustainability* 11:4018. <https://doi.org/10.3390/su11154018>
- Wang YR, Hessen DO, Samset BH, Stordal F (2022) Evaluating global and regional land warming trends in the past decades with both MODIS and ERA5-Land land surface temperature data. *Remote Sens Environ* 280: 113181. <https://doi.org/10.1016/j.rse.2022.113181>
- Wanishsakpong W, McNeil N (2016) Modelling of daily maximum temperatures over Australia from 1970 to 2012. *Meteorol Appl* 23(1):115-122. <https://doi.org/10.1002/met.1536>
- Wongsai N, Wongsai S, Huete A (2017) Annual seasonality extraction using the cubic spline function and decadal trend in temporal daytime MODIS LST data. *Rem Sens* 9(12):1254. <https://doi.org/10.3390/rs9121254>
- World Data (2022) Taiwan geography. <https://www.worlddata.info/asia/taiwan/index.php>. Accessed 27 October 2022